First-principles Calculation of Elastic and Electronic Structure Properties of Hexagonal Antiperovskite-type Carbides $XCCr_3$ (X=Al, Ga or Zn) Materials

David MAINA NJUGUNA[1*], Phillip OTIENO NYAWERE[2], and Elicah WABULULU[3]

[*1]*Department of Physical and Biological Sciences, Kabarak University, P.O. Box Private Bag – 20157 Kabarak, Nakuru, Kenya*

[1]*mainadavid964@gmail.com*

[2]*Department of Physical and Biological Sciences, Kabarak University, P.O. Box Private Bag – 20157 Kabarak, Nakuru, Kenya*

[2]*pnyawere@gmail.com*

[3]*Department of Natural Sciences, Catholic University of Eastern Africa, P.O. Box 62547, Nairobi, Kenya*

[3]*ewabululu@cuea.edu*

Submitted 18th January 2023, Accepted 20th February 2023 and Published 29th March 2023

ABSTRACT

Hexagonal chromium based Antiperovskite materials have been attracting a lot of research interest lately as a result of their superconducting properties. In this study the elastic and electronic structure properties of $XCCr_3$ (X= Al, Ga or Zn) were investigated using first principles density functional theory within the generalized gradient approximations using Quantum Espresso code. Shear Modulus (G), Young's Modulus (E), Bulk modulus (B), Poisson ratios (υ) and Zener anisotropy factor (A) values are calculated and evaluated in calculations of elastic properties. Mechanical stability and stiffness of these materials are determined and $XCCr_3$ (X= Al, Ga or Zn) compounds are found to be mechanically stable at zero pressure. The Fermi level locates at the vicinity of density of states (DOS) peak, which leads large DOS at the Fermi level $N(E_F)$ with values of 4.89, 5.72 and 4.32 states/eV for $AlCCr_3$, $GaCCr_3$ and $ZnCCr_3$ respectively. The band structures are similar to that of superconducting Antiperovskite $MgCNi_3$.

Key Words: Antiperovskite, Elastic, Mechanical stability

I.INTRODUCTION

Antiperovskite superconductors are among the materials that have attracted more attention in research because of the projected benefits they can deliver if better and efficient ones are discovered (Fortyn *et al.,* 2010; Gutfleisch *et al.,* 2011). This has motivated researchers and industrial users to improve the electronic structure and mechanical properties to achieve the conditions for better performance. Both theoretical and experimental methods have been embraced to achieve new discoveries in these efforts. The superconducting environment and other associated material properties greatly affect the performance of the superconductor towards realizing efficiency. Elastic behaviour of materials is one such property that affects superconductivity and is a true measure of how material deformations relate to external stress (Rivlin, 1997). The elastic behaviour is more important in determining how best materials can change due to intrinsic and extrinsic effects that affect the atomic orientation and structural geometry. This change is much dependent on the chemical composition, the structure of the crystal lattice, and the deforming stress. This work has therefore investigated the elastic and electronic structure properties of hexagonal Antiperovskite-type carbide materials in order to identify the one that is most suitable for better thermal conductivity.

The study of elastic properties of solids helps in analysing some of their vital properties such as anisotropy, ductility and brittleness. The elastic constants are used to show how dynamic and mechanical properties are connected in regard to the type of forces present in the solids. Much emphasis is put on the stiffness and stability of the material. The elastic constant also plays a major role in predicting the mechanical nature in solid-state physics. A hexagonal crystal has five independent elastic constants which are C_{11}, C_{12}, C_{13}, C_{33} and C_{44}. These constants are obtained by fixing the full energies of a strained crystal to a fourth-order polynomial strain (Pugh, 1954). The bulk modulus is used to measure the ability to resist deformation upon the application of pressure. A greater value of bulk moduli results into a greater capacity to resist deformation (Cherkaev & Gibiansky, 1993). Shear modulus measures the resistance to shear deformation on shear pressure.

Poisson's ratio which is a measure of stability of a crystal against shear ranges. The ratio usually varies between 0 and 0.5 (Chen, 2011). Pugh's ratio measures the ductility and brittleness of a material. The critical value for this ratio is given as 1.75. A value of less than 1.75 represents brittleness and a value above 1.75 indicate ductility (Liu, 2021). The necessary and sufficient conditions for mechanical stability criteria for hexagonal structures are given by the following conditions (Nye, 1985).

$$C_{11} > 0; C_{11} - C_{12} > 0; C_{44} > 0; (C_{11} + C_{12})C_{33} - 2C_{13}^2 > 0$$

The shear moduli *G* and bulk moduli *B* are given by equation (1) and (2) (Han *et al.,* 2008).

$$\boldsymbol{B = \frac{1}{3}(C_{11} + 2C_{12})} \quad (1)$$

$$\boldsymbol{G = \frac{1}{5}(3C_{44} + C_{11} - C_{12})} \quad (2)$$

The shear moduli and bulk moduli are also approximated by Voigt-Reuss-Hill (VRH) where the Voigt bounds of B_V and G_V are given by equation (3) and (4) (Davarpanah & Vasarhelyi, 2020).

$$\boldsymbol{B_V = \frac{2}{9}(C_{11} + C_{12} + \frac{1}{2}C_{33} + 2C_{33})} \quad (3)$$

$$\boldsymbol{G_V = \frac{1}{30}(7C_{11} - 5C_{12} + 12C_{44} + 2C_{33} - 4C_{13})} \quad (4)$$

And the Reuss bounds are given as;

$$B_R = \frac{(C_{11}+C_{12})C_{33}-2C_{13}^2}{C_{11}+C_{12}+2C_{33}-4C_{13}} \quad (5)$$

$$G_R = \frac{5}{2}\{\frac{[(C_{11}+C_{12})C_{33}-2C_{13}^2]C_{44}C_{66}}{3B_VC_{44}+[(C_{11}+C_{12})C_{33}-2C_{13}^2](C_{44}+C_{66})} \quad (6)$$

Using VRH, B and G are expressed as

$$B_{VRH} = \frac{1}{2}(B_V + B_R) \quad (7)$$

$$G_{VRH} = \frac{1}{2}(G_V + G_R) \quad (8)$$

Where the subscripts V and R are the Voigt and the Reuss forms respectively. The Young's moduli E, Poisson's ratio υ and anisotropic coefficient *A* are obtained according to equation. (9), (10) and (11) respectively (Khon, 1965; Music & Schneider, 2006).

$$E = \frac{9BG}{3B+G} \quad (9)$$

$$v = \frac{3B-2G}{2(3B+G)} \quad (10)$$

$$A = \frac{2C_{44}}{C_{11}-C_{12}} \quad (11)$$

Figure 1:

A schematic representation of the host crystal $AlCCr_3$ showing all the atomic positions.

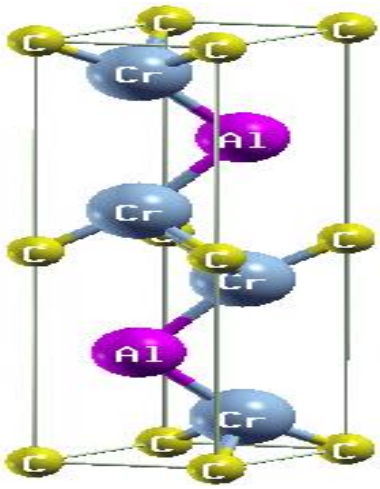

Source: Research Data, (2023)

II. METHODOLOGY

The density functional theory (DFT) has been successfully applied to the *ab-initio* calculations of the ground-state properties of materials (Hohenberg & Khon, 1964; Vanderbilt, 1990). In this study, first principles calculations were based on plane wave self-consistent field (PWscf) method as implemented in the Quantum Espresso Simulation package (Giannozzi *et al.*, 2009). The PWscf can lead to very accurate results comparable to other all-electron method. For the exchange correlation functional, the Generalized Gradient Approximation (GGA) according to Perdew–Burke–Ernzerhof (PBE) parameterization was used (Perdew, 1992). Optimized cell dimensions, the k-points, and the kinetic energy cut-off values were properly checked through graphing and accurate values were obtained at the convergence of the ground state energy at minimum convergence threshold in the calculation using the proper basis sets.

Calculations of Poisson ratios, young's modulus, Bulk and Shear Modulus (all in Voigt-Reuss-Hill approximations), Elastic constants, average Debye sound velocity, solid density and Debye temperature was done using Thermo_PW code interfaced with Quantum Espresso (Corso, 2018). In our calculations, the wave functions kinetic energy cut-off points were all set at 35 Ry and ecutrho set at 350 Ry. A smearing width of 0.01 Ry and convergence threshold of 1.0E-12 Ry with a mixing beta of 0.4 was applied. The K-points separation of 18x18x4 was used for all the compounds.

III. RESULTS

The elastic stability of a hexagonal crystal structure is determined using the elastic potential free energy equation;

$$\emptyset = \frac{1}{2}\boldsymbol{C_{ij}\varepsilon_i\varepsilon_j} \tag{12}$$

Where$\emptyset \geq 0$. When $\emptyset = 0$, we have equilibrium state and when $\emptyset > 0$, there is a state of mechanical deformation. This therefore requires that the principal minors of C_{ij} matrix given by eqn (13) must all be positive –definite.

$$C_{ij} = \begin{bmatrix} C_{11} & C_{12} & C_{13} & 0 & 0 & 0 \\ & C_{11} & C_{13} & 0 & 0 & 0 \\ & & C_{33} & 0 & 0 & 0 \\ & & & C_{44} & 0 & 0 \\ & & & & C_{44} & 0 \\ & & & & & X \end{bmatrix} \tag{13}$$

where $X = \frac{1}{2}(C_{11} - C_{12})$. The matrix is symmetrical about its leading diagonal (Ledbetter, 1977). Crystals of hexagonal class have 5 independent elastic constants but due to added relation in the matrix C_{ij} we get the element X which now defines a tetragonal crystal. The calculated eigenvalues of the stiffness matrix from equation (13) leads to the following four basic conditions called Born stability conditions for elastic stability of a hexagonal crystal (Liu, 2017).

$$\boldsymbol{C_{11} > 0; C_{11} > C_{12}; C_{44} > 0; (C_{11} + C_{12})C_{33} > 2C_{13}^2} \tag{14}$$

From Table 1, it can be noted that the values of elastic constants calculated satisfy the four born criterion conditions stated in equation (14). This therefore shows that the three structures studied in this work are elastically stable.

Table 1:
Elastic Constants in GPa

Material	C_{11}	C_{12}	C_{13}	C_{33}	C_{44}
$AlCCr_3$	243.2918	28.0521	21.5749	191.9535	116.5725
$GaCCr_3$	189.8909	27.7094	28.8399	178.0325	64.2360
$ZnCCr_3$	187.4470	21.6480	10.6917	105.5867	74.6348

A. Elastic Anisotropy

A material is said to be anisotropic if it displays properties with different values when measurements are taken along axes in different directions. The elastic anisotropy, denoted by A,

is used to determine how elastic properties of solids behave towards the direction of the stress (Sun *et al.*, 2004).

Hexagonal crystals have three shear-type anisotropy ratios defined by A_1, A_2 and A_3 respectively.

$$\boldsymbol{A_1} = \frac{\frac{1}{6}(\boldsymbol{C_{11}+C_{12}+2C_{33}-4C_{13}})}{\boldsymbol{C_{44}}} \quad (15)$$

$$\boldsymbol{A_2} = \frac{\boldsymbol{2C_{44}}}{(\boldsymbol{C_{11}-C_{12}})} \quad (16)$$

And

$$\boldsymbol{A_3} = \boldsymbol{A_1 A_2} = \frac{\frac{1}{3}(\boldsymbol{C_{11}+C_{12}+2C_{33}-4C_{13}})}{\boldsymbol{C_{11}-C_{12}}} \quad (17)$$

The shear-type anisotropy ratios derived from C_{ij} values and obtained using equations 15, 16 and 17 are given in Table 2.

Table 2:
Shear Type Anisotropic Ratios

Material	A_1	A_2	A_3
$AlCCr_3$	0.813	1.083	0.880
$GaCCr_3$	1.189	0.792	0.941
$ZnCCr_3$	0.843	0.900	0.758

When the elastic anisotropy ratio is $A = 1$, the crystal is isotropic. Otherwise values of A which are less than or greater than unity indicates anisotropy. The calculated shear anisotropic factors for the studied compounds are listed in Table 2. It is observed that all the materials under consideration are elastically anisotropic. Further, when $C_{33} > C_{11}$, the compounds are more incompressible along the C-direction than along the A-direction. From Table 1, it is noted that all the materials under study satisfies this condition.

Calculations of Poisson ratios 'ν', Young modulus 'E', Bulk modulus 'B' and Shear Modulus 'G' under Voigt and Reuss approximations as well as Voigt-Reuss-Hill average of the two approximations are presented in Table 3.

Bulk modulus is a measure of how a substance withstands changes in volume when compressed from all sides. The capacity of a material to resist deformation is directly proportional to its bulk modulus. From Table 3, it is observed that $GaCCr_3$ has the highest value of bulk modulus while $ZnCCr_3$ has the lowest value. The results clearly demonstrate that, of the three materials investigated in this work, $GaCCr_3$ has the strongest capacity to resist fracture.

Shear modulus is a numerical value that measures the ability of materials to resist transverse deformation. A larger value of shear modulus indicates that the solid is highly rigid and may require greater force to be deformed. The calculated results of shear modulus are presented in Table 3. Of the three compounds studied, $AlCCr_3$ has the largest value of shear modulus hence, the strongest capacity to resist plastic deformation.

Young modulus is a ratio that measures the tensile elasticity of a material. That is, a measure of the ability of a material to withstand variations in length when subjected to compression or lengthwise tension. It is obtained when longitudinal stress is divided by strain, which indicates how stiff a material is. The larger the ratio, the stiffer the material. From Table 3 it can be deduced that $AlCCr_3$ is stiffest of all the three materials studied.

Pugh's ratio is a measure of how ductile or brittle a material is. The critical value for this ratio is given as 0.5. A value of less than 0.5 represents brittleness and a value above 0.5 indicate

ductility. Considering this, the results in Table 3 show that the Pugh's ratios for all the three materials are above the critical value. This therefore implies that they are all ductile though $AlCCr_3$ is the most ductile.

Poisson's ratio is given by calculating the ratio of the lateral strain to that of the longitudinal strain in the direction of the stretching force. The ratio usually varies between 0 and 0.5. From Table 3, it can be noted that all the three materials are brittle though the Poisson's ration for $GaCCr_3$ is higher than the rest.

Table 3:

Bulk Modulus and Shear Modulus in GPa under Voigt, Reuss and Hill Averaging Scheme, Young's Modulus in GPa, Poisson's Ratio and Pugh Ratio (G_H/B_H)

Material	B_V	B_R	B_H	G_V	G_R	G_H	E	Y	G_H/B_H
$AlCCr_3$	59.5703	58.9179	59.2441	123.7460	122.7039	123.2249	218.3139	0.114	2.079
$GaCCr_3$	80.9547	80.8989	80.9268	73.4075	72.5693	72.9884	168.3517	0.153	0.901
$ZnCCr_3$	43.8242	41.1625	42.4933	85.6642	81.7713	83.7178	151.5951	0.094	1.970

B. Debye Temperature

As a fundamental parameter, the Debye temperature correlates with many physical properties of solids, such as specific heat, elastic constant and superconducting temperature (Ravindran *et al*, 1998). One of the standard methods to calculate the Debye temperature can be estimated from the averaged sound velocity (Zhang *et al.*, 2007).

The average sound velocity V_M is approximately given by equation (18) (Jiang *et al.*, 2019).

$$\boldsymbol{V_m = \left[\frac{1}{3}\left(\frac{2}{v_t^3} + \frac{1}{v_l^3}\right)\right]^{-1/3}} \quad (18)$$

Where v_l and v_t are the longitudinal and transverse sound velocities which can be obtained from bulk modulus B and shear modulus G (Wang & Ye, 2003).

$$\boldsymbol{V_l = \left(\frac{3B+4G}{3\rho}\right)^{1/2}} \quad (19)$$

$$\boldsymbol{V_t = \left(\frac{G}{\rho}\right)^{1/2}} \quad (20)$$

The values of Debye temperature are estimated using equation (21).

$$\boldsymbol{\Theta_D = \frac{h}{k_B}\left[\frac{3nN_A\rho}{4\pi M}\right]^{-1/3} V_M} \quad (21)$$

Where V_M is the average sound velocity, h, k_B and N_A are planks constant, Boltzmann constant and Avogadro number respectively. ρ is the density, M is the molecular weight and n is the number of atoms in the unit cell. From Table 4, the Debye temperatures for $AlCCr_3$, $GaCCr_3$ and $ZnCCr_3$ were found to be 718.557K, 483.170K and 509.329K respectively. This result indicates that $AlCCr_3$ has the highest Debye temperature implying that it has the highest interatomic bonding, the highest melting point, greatest hardness and highest thermal conductivity than the rest.

Table 4:

Compressional (V_P), Bulk (V_B), Shear (V_G), Average Debye (V_D), Sound Velocities in m/s, Solid Density (ρ) in g/cm^3 and Debye Temperature (θ_D) in Kelvin Calculated by Voigt-Reuss-Hill Average

Material	V_P	V_B	V_G	V_D	ρ (g/cm^3)	Θ_D(K)
$AlCCr_3$	6790.410	3495.724	5041.546	5416.127	5.434	718.557
$GaCCr_3$	5340.797	3598.687	3417.627	3750.006	5.598	483.170
$ZnCCr_3$	5001.938	2626.477	3686.564	3940.871	5.510	509.329

C. Electronic structure properties

The calculated band structure of $XCCr_3$ (X= Al, Ga or Zn) with FM spin configuration along high symmetry direction in the BZ at the ambient pressure is shown in Figure 2. The Fermi level (E_F) is set at zero and indicated by a coloured line. The band structures in figure 2 of the three compounds are very similar. Bands from -15eV to -12eV are mainly from the C-2s and Cr-3d states and the Cr-3d states contribute dominantly to the bands, which suggests the itinerant nature of Cr-3d electrons. The important notable point is that the overlaps on top of up- and down-spin states almost at every level are visible. To better understand the nature of the electronic band structure of $XCCr_3$ (X= Al, Ga or Zn), we have calculated density of states, which are shown in Figure 3. It is observed that, the Fermi level locates at the vicinity of the DOS peak, which leads large DOS at the Fermi level N(E_F) with values of 4.89, 5.72 and 4.32 states/eV for $AlCCr_3$, $GaCCr_3$ and $ZnCCr_3$ respectively.

Figure 1:

The Band Structures for (a) $AlCCr_3$, (b) $GaCCr_3$ and (c) $ZnCCr_3$

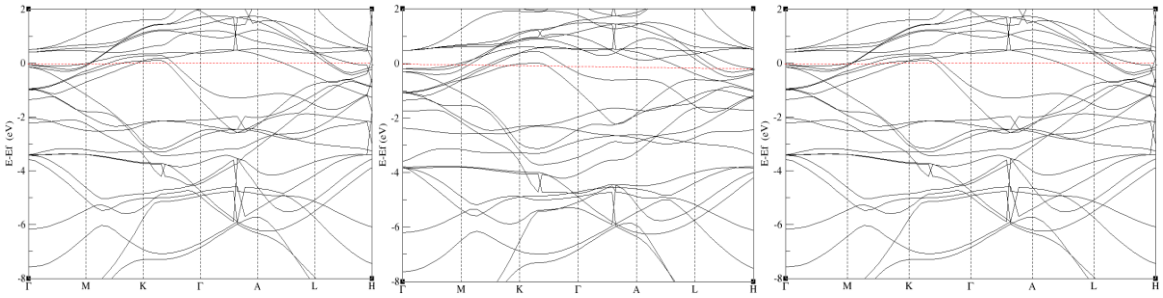

(a) (b) (c)

Figure 2:
Density of States of (a) $AlCCr_3$, (b) $GaCCr_3$ and (c) $ZnCCr_3$

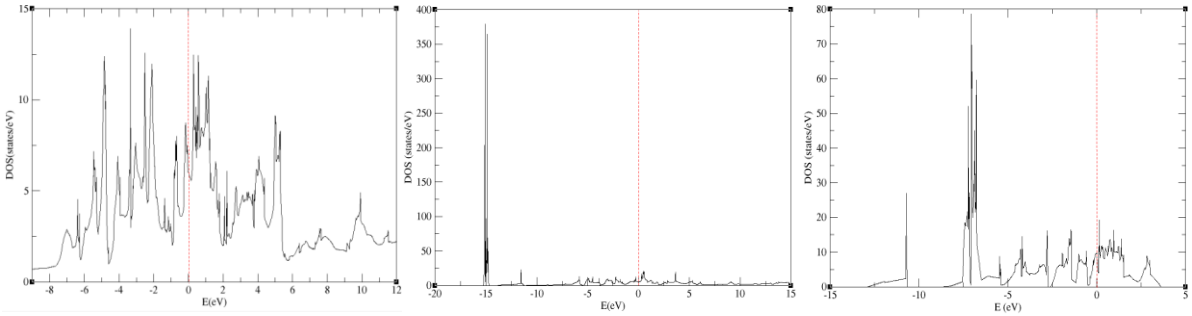

(a) (b) (c)

IV. DISCUSSION

This study was aimed at determining the elastic and electronic structure properties of hexagonal Antiperovskite-type carbides $XCCr_3$ (X=Al, Ga or Zn) Materials. The values of elastic constants calculated satisfy the four Born and Huang conditions and the materials were elastically stable. The calculated shear anisotropic factors show that the materials are elastically anisotropic. It is observed that $GaCCr_3$ has the highest value of bulk modulus while $ZnCCr_3$ has the lowest value. It was deduced that $AlCCr_3$ is stiffest of all the three materials studied. It is noted that all the three materials are brittle though the Poisson's ration for $GaCCr_3$ is higher than the rest. The calculated Debye temperatures for $AlCCr_3$, $GaCCr_3$ and $ZnCCr_3$ were found to be 718.557K, 483.170K and 509.329K respectively. This study was unable to compare these results with any other since none was existing. Nonetheless, it can be easily seen that $AlCCr_3$ has the highest Debye temperature implying that it has the highest interatomic bonding, the highest melting point, greatest hardness and highest thermal conductivity than the rest. It is observed that, the Fermi level locates at the vicinity of the DOS peak, which leads large DOS at the Fermi level $N(E_F)$ with values of 4.89, 5.72 and 4.32 states/eV for $AlCCr_3$, $GaCCr_3$ and $ZnCCr_3$ respectively.

V. CONCLUSION

In this work, first principles DFT using Thermo_PW interfaced with Quantum Espresso Code was used to investigate the elastic properties and the mechanical stability of hexagonal $XCCr_3$ (X= Al, Ga or Zn). The calculated values for elastic constants for all the materials were found to be in line with the Born and Huang conditions for mechanical stability. In addition, the values of the elastic constants were relatively high indicating that the materials studied had good resistance against deformation. The materials are also good thermal conductors deduced through their Debye temperature. This study conclusively shows that the three compounds are ductile in nature and they may have similar thermal properties. Similar to superconducting $MgCNi_3$, there are electron and hole bands that cross the Fermi level indicating multiple-band natures. Fermi level is located at the vicinity of the DOS peak, which leads large DOS at the Fermi level $N(E_F)$ dominated by Cr-3d electrons. These similarities in band structures possibly indicate that $AlCCr_3$, $GaCCr_3$ and $ZnCCr_3$ have superconductivity nature, which needs to be further investigated from experimental and theoretical studies.

VI. RECOMMENDATIONS

The study only dealt with theoretical findings on elastic and electronic structure properties of $XCCr_3$ (X=Al, Ga, Zn). Experimental study of the hexagonal $XCCr_3$ (X=Al, Ga, Zn) is recommended. The similarities in band structures possibly indicate that $AlCCr_3$, $GaCCr_3$ and $ZnCCr_3$ have superconductivity nature, which needs to be further investigated from experimental and theoretical studies.

VII. ACKNOWLEDGMENTS

The authors are very grateful to the Centre for High Performance Computing (CHPC), South Africa for providing the computational resources which led to the success of this study.

VIII. REFERENCES

Chen, X., Niu, Q., Li, H., & Li, Y. (2011). Modeling hardness of polycrystalline materials and bulk metallic glasses. *Intermetallic, 19*(9), 1275-1281.

Cherkaev, A., & Gibiansky, H. (1993). Coupled estimates for the bulk and shear moduli of a two-dimensional isotropic elastic composite. *Journal of the Mechanics and Physics of Solids, 41*(5), 937-980.

Corso, A. D. (2018). The International School for Advanced Studies. J*ournal of Applied Physics, 12*, 65-78.

Davarpanah, S. M., Van, P., & Vasarhelyi, B. (2020). Investigation of the relationship between dynamic and static deformation moduli of rocks. *Geomechanics and Geophysics for Geo-Energy and Geo-Resources, 6*(1), 1-14.

Fortyn, S. R., Leonard. J. L., MacManus, L., & Quanxi, J. (2010). Materials science challenges for high-temperature superconducting wire. *Peer Reviewed Artic*le, 299–310.

Giannozzi, P., Baroni, S., Bonini, N., Calandra, M., Car, R., Cabazon, C., & Wentzcovitch, R. M. (2009). A modular and open-source software project for quantum simulations of materials. *Journal of Physics: Condensed Matter, 21*(39), 395-502.

Gutfleisch, O., Willard, M. A., Bruck, E., Chen, C. H., Sankar, S. G., & Liu, J. P. (2011). Magnetic materials and devices for the 21st century: Stronger, lighter, and more energy efficient. *Advanced Mater, 23*(8), 21–42.

Han, M., & Miller, G. J. (2008). An application of the Coloring Problem: Structure Composition Bonding Relationships in the Magnetocaloric Materials. *Inorganic Chemistry, 47*(2), 515-528.

Hohenberg, P., & Khon, W. (1964). Inhomogeneous Electron Gas. *Physical Review*, 136-864.

Jiang, D., Wu, M., Liu, D., Li, F., Chai, M., & Liu, S. (2019). Structural stability, electronic structures, mechanical properties and Debye temperature of transition metal impurities in Tungsten: A first-principles study. *Journal of Metals, 9*(9), 59-67.

Khon, W., & Sham, L. J. (1965). Self-Consistent Equations Including Exchange and Correlation Effects. *Physics Review, 140,* 11-33.

Ledbetter, H. M., (1977). Elastic properties of zinc: A compilation and a review. *Journal of Physical and Chemical Reference Data, 6* (4), 1181-1203.

Liu, H., Tang, G., Ma, S., Li, Y., & Liang, C. (2021). Short range ordering governs brittleness and ductility in W-Ta solid solution: Insights from Pugh's shear-to-bulk modulus ratio. *Scripta Materialia, 204*, 114-136.

Liu, Z., Li, H., Fan, C., & Lou, W. (2017). Necessary and sufficient elastic stability conditions in 21 quasicrystal Laue classes. *European Journal of Mechanics, 65,* 30-39.

Music, D., & Schneider, J. M. (2006). Elastic properties of MFe_3N (M= Ni, Pd, Pt.) studied by ab initio calculations. *Applied Physics Letters, 88*(3), 31-91.

Nye, J. F. (1985). Physical properties of crystals: Their representation by tensors and matrices. *Oxford University Press, 42*(1), 583-599.

Perdew, J. P., Chivalry P., & Vosko, S. (1992). Atoms, molecules, solids, and surfaces: Applications of the generalized gradient approximation for exchange and correlation. *Physical Review, 46,* 66-71.

Pugh, S. F. (1954). Relations between the elastic moduli and the plastic properties of polycrystalline pure metals. *Journal of Science, 45*(367), 823-843.

Ravindran, P., Fast, L., Korzhavyi, P. A., Johansson, B., Wills, J., & Eriksson, O. (1998). Density functional theory for calculation of elastic properties of orthorhombic crystals: Application to $TiSi_2$. J*ournal of Applied Physics,* 4891–4904.

Rivlin, R. S. (1997). Large elastic deformations of isotropic materials collect. *Journal of Physics, 822,* 109–199.

Sun, Z., Li, S., Ahuja, R., & Schneider, J. M. (2004). Calculated elastic properties of M_2AlC (M= Ti, V, Cr, Nb and Ta). *Solid State Communications, 129*(9), 589-592.

Vanderbilt, D. (1990). Soft self-consistent pseudopotentials in generalized eigenvalue formalism. *Physical review, 41*(11), 78-92.

Wang, S. Q., & Ye, H. Q. (2003). Ab initio elastic constants for the ionsdaleite phases of C, Si and Ge. *Journal of Physics, 23,* 53-67.

Zhang, J. M., Zhang, Y., Xu, K. W., & Ji, V. (2007). Young's modulus surface and Poisson's ratio curve for cubic metals. *Journal of Physics, 68,* 503–510.